



Buckling Analysis of a Thin-Walled C-Section Channel under Mechanical and Thermal Load

Omar Shabbir Ahmed¹, Abdul Aabid², Jaffar Syed Mohamed Ali^{1,*}, Meftah Hrairi¹, Norfazrina Mohd Yatim¹

¹ Department of Mechanical and Aerospace Engineering, Faculty of Engineering, International Islamic University Malaysia, P.O. Box 10, 50725 Kuala Lumpur, Malaysia

² Department of Engineering Management, College of Engineering, Prince Sultan University, PO BOX 66833, 11586 Riyadh, Saudi Arabia

ARTICLE INFO

Article history:

Received 7 May 2023

Received in revised form 12 July 2023

Accepted 21 July 2023

Available online 1 August 2023

Keywords:

Buckling Analysis; thin-walled structures; C-section channel; finite element method; critical buckling load factor

ABSTRACT

Buckling analysis of thin-walled structures is essential to ensure their structural integrity under various loading conditions. The study aims to analyse buckling in thin-walled structures, particularly a C-section channel, under different loads, considering cases with and without holes, using FEM. It investigates hole impact on buckling, critical load, and mode shapes, offering insights for C-section channel design. A finite element method (FEM) is used to model the structure and simulate mechanical and thermal loading conditions. Additionally, the study investigates the critical buckling load factor and mode shapes for both cases with and without holes. The results show that the presence of holes significantly affects the buckling behaviour of the structure. The mode shapes indicate that the buckling behaviour of the structure is different for each case. The critical buckling load factor is lower for the C-section channel with holes, indicating a higher risk of buckling. The results of this study provide insights into the buckling behaviour of thin-walled structures and demonstrate the importance of considering the presence of holes in the design and optimization of C-section channels.

1. Introduction

Thin-walled structures are widely used in aerospace [1,2], automotive, and civil engineering applications [3]. These structures are prone to buckling under compressive loads, which can lead to catastrophic failures [4]. Therefore, it is crucial to study the buckling behaviour of thin-walled structures under different loading conditions to ensure their safe and efficient design. One of the critical issues that engineers face while designing these structures is their buckling behaviour. Under thermal loads, thin-walled structures may experience buckling that could lead to critical failures. Therefore, understanding the buckling behaviour of thin-walled structures under thermal loads is crucial. This literature review summarizes some of the recent studies on buckling analysis of thin-walled structures under mechanical and thermal load.

* Corresponding author.

E-mail address: jaffar@iium.edu.my

<https://doi.org/10.37934/aram.109.1.116>

Zhu *et al.*, [5] analysed the buckling behaviour of thin-walled structures and showed that the buckling behaviour of these structures is affected by their cross-sectional shape and aspect ratio. Ma *et al.*, [6] investigated the buckling behaviour of thin-walled structures under combined axial and bending loads and showed that the buckling load of thin-walled structures is lower than that under purely axial loads. Wang *et al.*, [7] studied the buckling behaviour of thin-walled structures under axial compression load. The authors used the finite element method to analyse the buckling behaviour of different thin-walled structures. The study showed that the buckling behaviour of these structures depends on their geometrical parameters and material properties. The influence of manufacturing on the buckling performance of thin-walled, channel-section CFRP composites has shown by the authors Czapski and Lunt [8] through the experimental and simulation approach that useful to define composite materials for structural performance. Improved the brittle flexural behaviour of composite laminates finding traditional laminates based on the type of structural application [9]. A review has been made on composite laminates for thin-walled structures and shown the challenges in current industry [10].

Kumar *et al.*, [11] used the finite element method to analyse the buckling behaviour of different thin-walled structures and showed that the buckling behaviour of these structures under dynamic loading is affected by the loading frequency and amplitude, and the critical buckling mode may change under dynamic loading. Guo *et al.*, [12] showed that the presence of a cut-out in a thin-walled structure significantly affected the buckling behaviour of the structure under thermal loads. Seidi *et al.*, [13] studied the buckling behaviour of thin-walled structures under thermal loading. The authors used the finite element method to analyse the buckling behaviour of different thin-walled structures, including cylindrical shells, conical shells, and spherical shells. The study showed that the buckling behaviour of these structures under thermal loading is different from that under mechanical loading, and the buckling load is affected by the material properties and boundary conditions. Han [14] derived the buckling load and critical buckling mode of the cylindrical shell and showed that the buckling load of the cylindrical shell under thermal loads was lower than that under mechanical loads. Kadoli and Ganesan [15] considered a rectangular tube and a cylindrical shell made of aluminium alloy and subjected them to thermal loads and showed that the buckling behaviour of the structures was significantly affected by the thermal load.

Kim *et al.*, [16] analysed the buckling behaviour of a thin-walled beam subjected to bending using analytical and numerical methods. The authors considered the effect of different boundary conditions and loading conditions on buckling behaviour. Nguyen *et al.*, [17] investigated the buckling behaviour of a thin-walled cylindrical shell under external pressure using experimental and numerical methods. The study showed that the buckling behaviour was influenced by the shell's geometrical parameters and the loading conditions. Shan *et al.*, [18] considered the effect of different boundary conditions on buckling behaviour and analysed the stress and deformation patterns of the structure. Zhao *et al.*, [19] analysed the buckling behaviour of a thin-walled cylindrical shell under torsion using the finite element method. The authors considered the effect of the shell's curvature on the buckling behaviour and compared the results with those of previous studies. Jiao *et al.*, [20] investigated the buckling behaviour of a thin-walled cylindrical shell under axial compression using an experimental method. The study showed that the initial imperfection of the shell had a significant influence on the buckling behaviour [21] and the critical buckling load.

The studies reviewed suggest that the buckling behaviour of thin-walled structures under mechanical [4] and thermal loads is significantly affected by various factors, including the material properties, the presence of cut-outs or holes [22], the boundary conditions, and the aspect ratio of the structure. The results from the energy method and the finite element method are generally consistent in predicting the buckling behaviour of thin-walled structures under mechanical and

thermal loads. The buckling analysis of thin-walled structures, such as the study of C-section channel behaviour under mechanical and thermal loading with and without holes using finite element methods, is essential under modern conditions to enhance structural integrity, optimize design, and mitigate buckling risks for various applications. The results of these studies can provide practical insights for optimizing the design and ensuring the structural integrity of thin-walled structures, particularly C-section channels, by understanding the effects of mechanical and thermal loading, as well as the presence of holes, on buckling behaviour and critical load factors. Further research is needed to develop more accurate and efficient methods for analysing the buckling behaviour of thin-walled structures under different loading conditions. The current study aims to demonstrate that the buckling behaviour of thin-walled structures is influenced by various factors, including loading conditions, geometrical parameters, material properties, boundary conditions, and the presence of cut-outs. The numerical methods used to investigate buckling behaviour in these studies provide insight into the underlying physics and can help engineers design more robust and efficient structures.

2. Problem Definition

The objective of this study is to perform a buckling analysis of a thin-walled C-section channel under mechanical and thermal loading, considering both the cases with and without holes. The C-section channel is a commonly used structural component in various engineering applications and can be subjected to different loading due to exposure in different environments.

The first part of the study will focus on creating a finite element model of the C-section channel with and without holes using a 3D finite element method. The mesh size and quality will be optimized to ensure accurate results. The material properties of the thin-walled structure will be defined, including the coefficient of thermal expansion, and other properties. The second part of the study will focus on defining the boundary conditions to simulate the structure's different loading conditions and support conditions. The boundary conditions will include constraints, loads, and initial conditions. The types of loads applied to the structure will depend on the type of buckling being analysed, such as critical buckling load and critical thermal load. The third part of the study will involve solving the finite element equations using numerical methods to obtain the temperature and displacement fields. The solution obtained will be used to determine the critical buckling load factor and mode shapes for both cases with and without holes in the C-section channel.

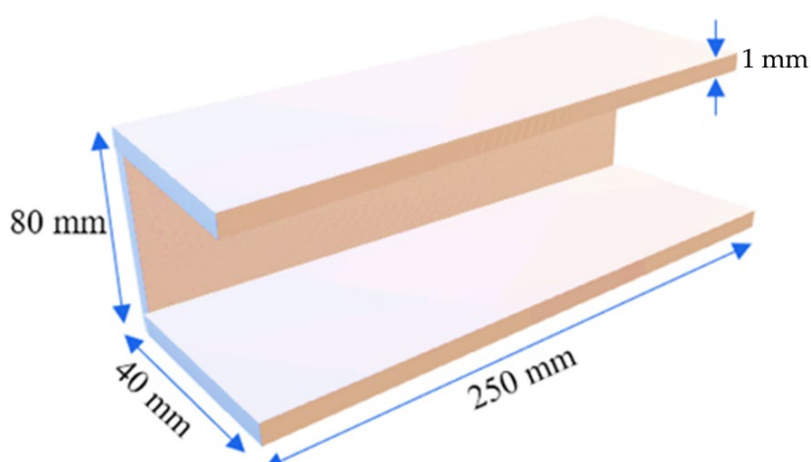


Fig. 1. A model description with its dimension

Finally, the results will be post-processed to compare the buckling behaviour of the C-section channel with and without holes. The mode shapes will be used to identify the type of buckling that occurred in the structure under thermal load. The buckling load factor will be used to determine the safety factor and whether the structure is in danger of buckling or not. This study will contribute to the understanding of the buckling behaviour of thin-walled structures under mechanical and thermal loading and provide useful insights for the design and optimization of C-section channels in various engineering applications.

3. Methodology

FEM for buckling analysis of a thin-walled structure under mechanical and thermal load was considered in the present work and it is a powerful numerical technique used to solve complex engineering problems that cannot be easily solved using analytical methods.

3.1 Geometry and Modelling

First, a finite element model of the thin-walled structure is created using a 3D ANSYS workbench software, and the model is then discretized into smaller elements using meshing options. The mesh size and quality are critical parameters that can significantly affect the accuracy of the results. Figure 1 shows the dimensions of the model which is designed as a c-section channel. The material used in the model is glass fibre-reinforced polymer (GFRP) which is represented in the model dimension as a channel with 80 mm height, 40 mm width, and a length of 250 mm. The flanges and web of the channel were composed of eight layers of 0.26 mm laminated sheets and had a thickness of 1 mm (0.125 mm each layer).

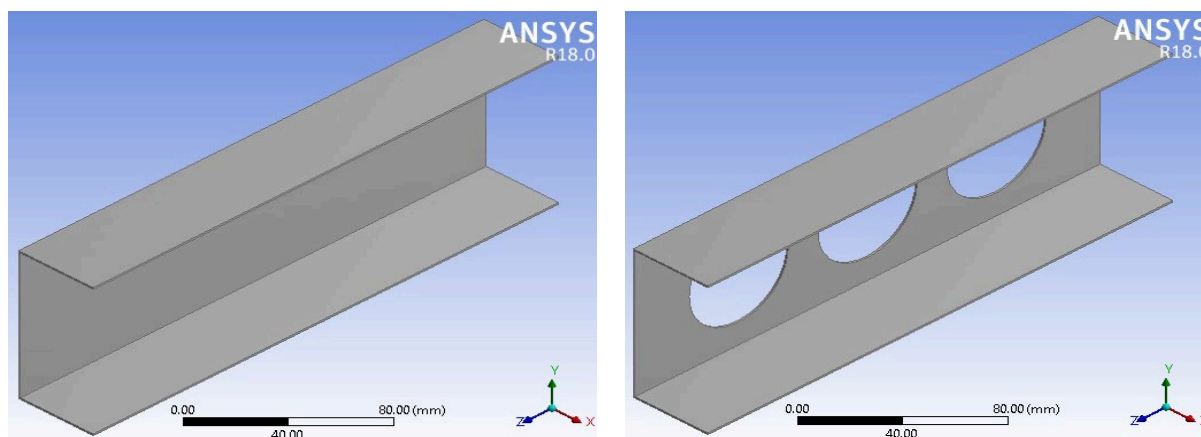


Fig. 2. A FE model without and with holes

Three parameters were investigated in this study: the spacing ratio, the shape of the hole, and the ratio of the opening (Figure 3). Each parameter was examined with three different configurations [22].

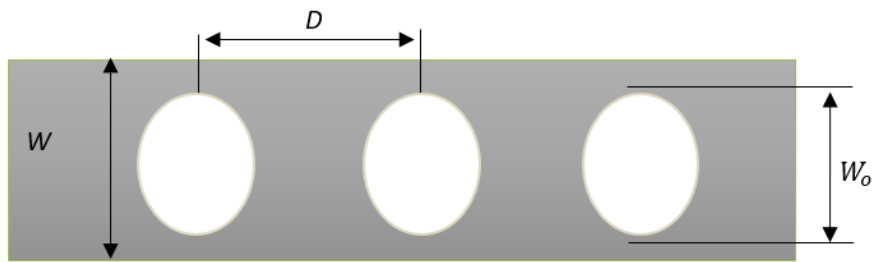


Fig. 3. Description of opening and spacing ratio

3.2 Material Properties

The mechanical properties of the material are defined in the finite element (FE) analysis software. Mechanical properties such as Young's modulus, Poisson's ratio, and shear modulus are used to define the constitutive equations that relate the stresses and strains in the material. Next, the material properties of the thin-walled structure are defined including the coefficient of thermal expansion. These properties are used to define the mechanical and thermal behaviour of the material when subjected to mechanical and thermal loading. The type of laminate considered quasi-isotropic and were analysed using the same thickness of each layer. This laminate type quasi-isotropic [+45/+45/+45/+45]_s was introduced into ANSYS benchwork software with their respective properties. The GFRP material used in the analysis had a mass density of 2200 kg/m³, and Table 1 lists the strength properties of the GFRP strut.

Table 1
 GFRP properties used for simulation

E1 (MPa)	E2(MPa)	ν	G12(MPa)	G13(MPa)	G23(MPa)
38000	8100	0.27	2000	2000	2000

3.3 Boundary conditions and meshing

A mesh with a size of 2 mm was selected based on the results of the mesh sensitivity analysis. The bottom end of the column was fixed-fixed, and all points in that section had restrained rotations (ROTX, ROTY, ROTZ) and translations (UX, UY, UZ). The load was applied to the upper part of the column at a specific reference point shown in Figure 4. The reference point at the bottom was identified as RP-1, while RP-2 was assigned to the top section.

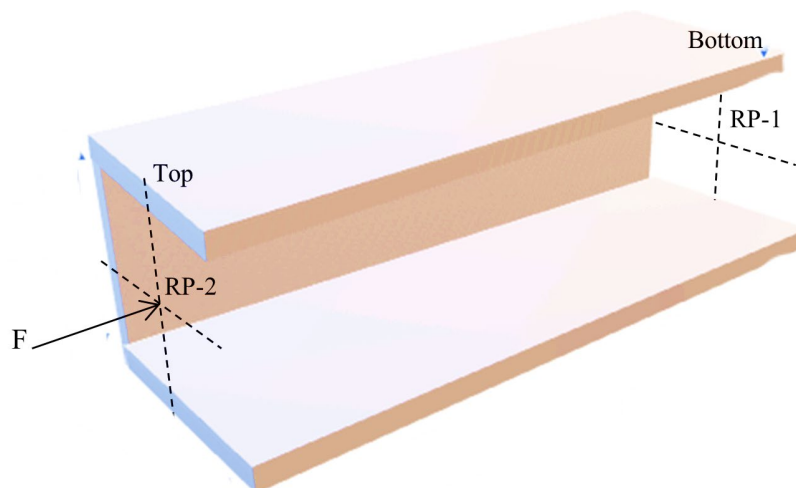


Fig. 4. Loading conditions on the model

The buckling analysis of the linear perturbation procedure in the postprocessor of the ANSYS workbench was used for the elastic buckling analysis. All models utilize multi-layered, QUAD4, and SHELL181. SHELL181 is a four-node with six degrees of freedom. This element expresses thin-walled structure geometry by a flat finite element degenerated from 3D finite element formulations of the structure's mid-surface [23]. The upper end's x , y , and z rotation angles were all assumed to be constrained (Figure 5). The vertical z -axis was set to be unrestricted while all degrees of freedom were restrained at the bottom end at the reference point. Using rigid body-pin (node) constraints, a uniform load was applied to a reference point representing the strut's upper nodes. The contact of the strut with the top plate is represented by this type of constraint. The FE model was given a nominal compressive load of 1.0 N. A linear eigenvalue buckling problem was used to determine the critical buckling load. The first buckling mode, which is referred to as the critical buckling load, was used in this study to generate the buckling mode shapes.

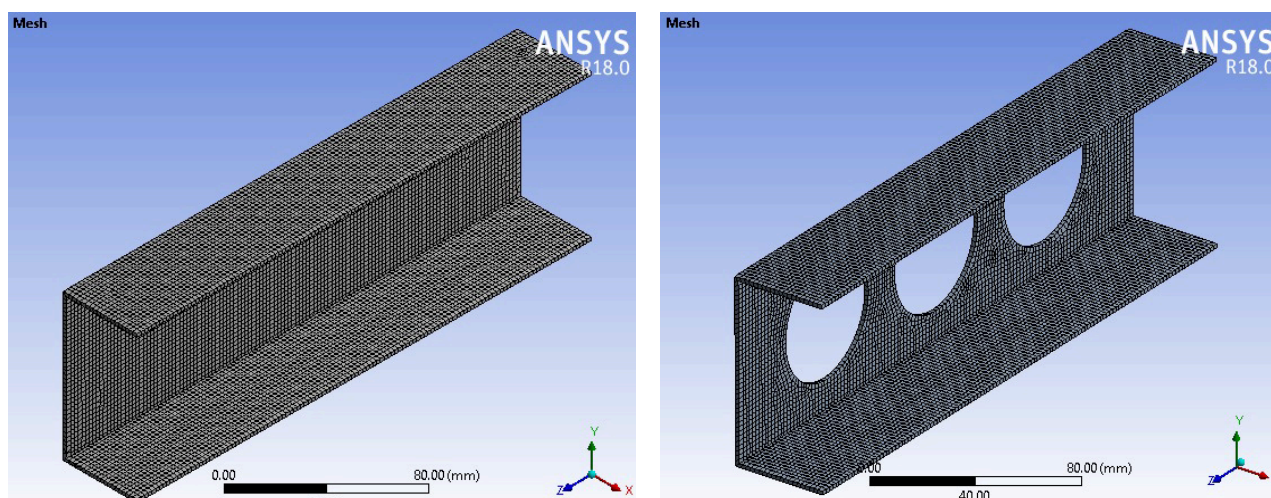


Fig. 5. FE mesh model without and with holes

3.4 Solution

The finite element equations are solved using numerical methods, such as the direct or iterative method, to obtain the temperature and displacement fields. The solution obtained will be the buckling load factor and mode shapes. The results are then post-processed to obtain the critical buckling load factor and mode shapes. The mode shapes are used to identify the type of buckling that occurred in the structure under thermal load. The buckling load factor is used to determine the safety factor and whether the structure is in danger of buckling or not.

The thermal critical buckling load is the load at which a column will buckle due to thermal expansion. It can be determined by performing a linear buckling analysis on the column, with the thermal loading applied as a uniform temperature change. We are going to determine the thermal critical buckling load on a column when the column is subjected to the increase in the temperature of 150°C from the room temperature which is 22°C , we are obtaining the load multiplier factor.

- i. **Linear Buckling Analysis:** Perform a linear buckling analysis on the model. This involves solving for the eigenvalues (load multiplier factors) and eigenvectors (buckling modes) of the system. The load multiplier factors represent the critical buckling loads as multiples of the applied load.

- ii. **Thermal Loading (T-critical):** Apply the thermal loading to the model. simulate the temperature increase from 22°C to 150°C. Incorporate the temperature-dependent material properties, including coefficients of thermal expansion.
- iii. **Eigenvalue Extraction:** Extract the lowest eigenvalue from the analysis. This corresponds to the most critical buckling mode and provides the load multiplier factor associated with the thermal critical buckling load.
- iv. **Interpretation:** The load multiplier factor indicates how much the applied load needs to be multiplied by to reach the critical buckling load under the specified.

4. Results and Discussion

4.1 FE Model Validation

To validate the proposed finite element (FE) model, this study relied on the buckling outcomes reported by Doan and Thai [23]. The length and cross-sectional dimensions of the specimen were matched and replicated to verify the accuracy of the current work. The buckling behaviour of both quasi-isotropic laminate and angle-ply laminate FE models was compared with their respective numerical analysis results to assess the reliability of the proposed model. The stacking sequences used were [0/+45/+45/+45/+45]_s for the quasi-isotropic laminate. Initially, the beam model without any holes was compared for both laminates to ensure higher reliability. The comparison of the critical buckling load's numerical results with a previous study is presented in Table 2.

Table 2
 Comparison of c-section model under mechanical load

Laminate Types	Critical Buckling Load (N)			Percentage error (%)
	Previous study [12]	ABAQUS [4]	Present work ANSYS	
Quasi-isotropic	10500 N	11201.2 N	10237.8 N	± 2.56 % and ± 8.6 %
-	-	8551 N	8625.8 N	± 0.86

Another validation of current model under thermal load has been compared with theoretical and numerical results [24]. The authors compared the FE result for first mode with theoretical solution available in the University of Connecticut for isotropic materials. The development of the FE model is grounded in previous research that examined an FRP composite thin rectangular plate. The plate has in-plane dimensions, with a length of 2 m and a width of 1 m. The plate's thickness is determined based on the length-to-thickness ratio ($s = a/t$) and is varied for a specific case. Stacking sequences were used symmetric quasi-isotropic (90/45/-45/0/0/-45/45/90). The comparison is provided in Table 3.

Table 3
 Comparison of c-section model under thermal load

Laminate Type	Critical Buckling Temperature (°C)		Percentage error (%)
	Theoretical [24]	Numerical (Current)	
Quasi-isotropic	28.2 °C	25.8 °C	± 8.5 %

4.2 Mesh Convergence Study

A mesh convergence study is conducted to assess the accuracy of the mesh in a current model. The study focuses on a basic model without any cut-outs in the c-section channel. To explore the impact of different mesh sizes, five element sizes ranging from 1.8 mm to 3 mm are tested. The

element size that produces the most similar results is selected for further analysis. The mesh refinement is then examined in relation to a specific case in the current work, which is similar to a previous study [23]. The accuracy of results using the FEM improves with smaller element sizes. In the mentioned scenario, achieving a more precise outcome with a 1.8 mm element size is valid; however, it's important to note that smaller elements increase the number of elements and nodes, demanding a higher PC configuration and longer runtime. The analysis determines that an element size of 2 mm closely aligns with the reference value and exhibits the lowest error, resulting in convergence of the results (Table 4). Thus, for this study, the optimal choice is a 2 mm element size, which strikes a balance between accuracy and computational efficiency, demonstrating a minor difference/error in critical buckling load compared to the 1.8 mm element size. This mesh size is subsequently employed for all models, with slight modifications near the holes of the structure to ensure smoother boundaries.

Table 4
 Mesh convergence study for c-section without cut-outs

Sl. No	Element size	No. of elements	No. of nodes	Critical buckling value
1	1.8	24777	25891	9001.5
2	2	20486	21389	9032.7
3	2.4	14199	16002	9082.8
4	3	9281	10281	9164.3

4.3 Total Deformation

The results obtained from the ANSYS simulation provide evidence that the inclusion of apertures diminishes the capacity of a beam to withstand an axial load prior to failure. The eigenvalue depicted in Figures 6 to 12 illustrates the critical buckling load and the thermal critical buckling load that these models can sustain before experiencing buckling. Figure 6 displays the eigenvalues in a C-section channel without any apertures, indicating that these eigenvalues should be higher compared to the C-section channel with apertures. To emphasize strength and reduce weight, the channel incorporates apertures and is subsequently tested with various shapes and sizes, as depicted in Figures 6 to 12.

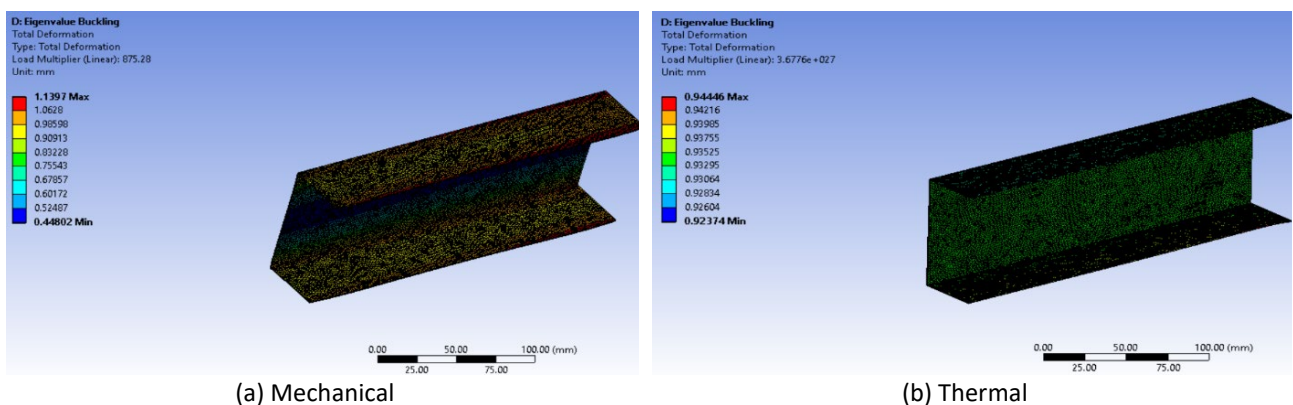


Fig. 6. Total deformation (Eigenvalue buckling) without cut-outs

The contours have been extracted independently for mechanical and thermal loads, as the eigenvalues exhibit significant variations between these two conditions. While the deformation phenomenon between the two cases is approximately similar and behaves in a consistent manner,

the presence of cut-outs in the C-sectional channel leads to a decrease in the buckling load results. This reduction in buckling load is clearly visible in the plots presented in the following section.

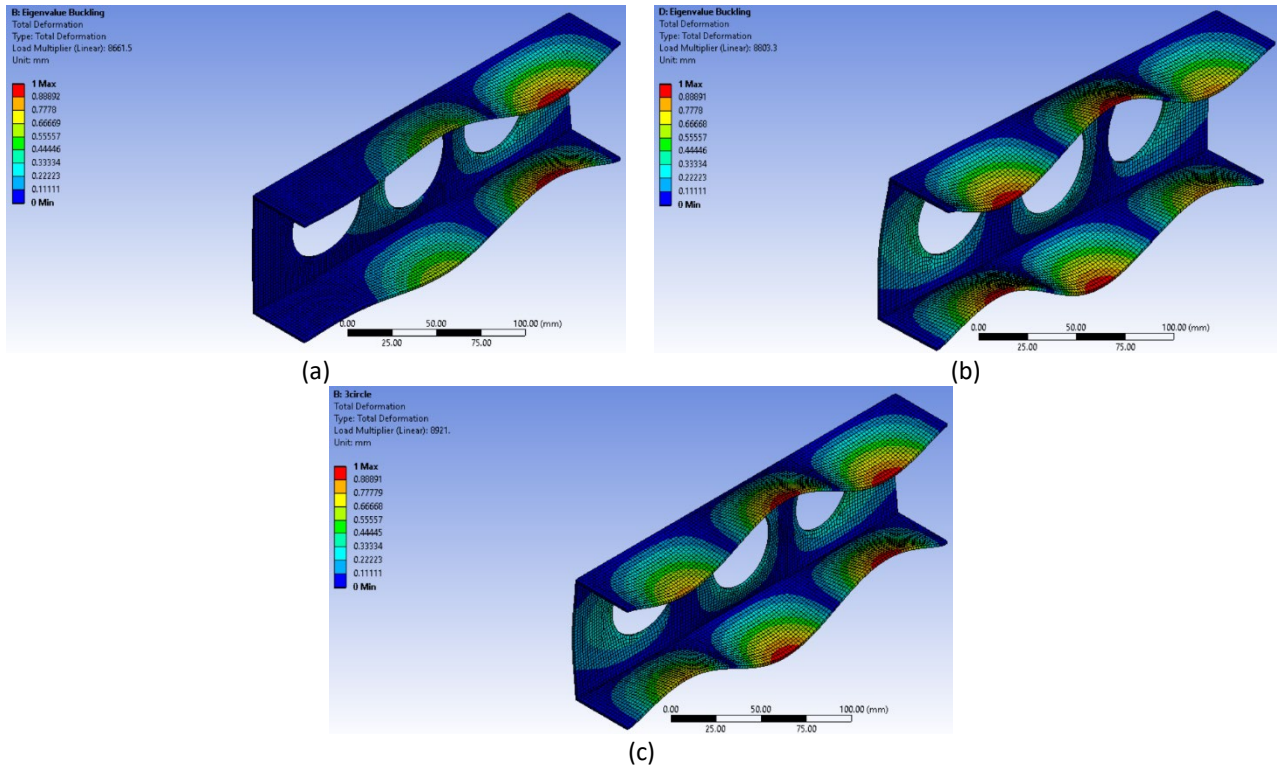


Fig. 7. Total deformation (Eigenvalue buckling) under mechanical load for circular cut-outs (a) $W/W_o= 1.5$ (b) $W/W_o= 1.6$ (c) $W/W_o= 1.7$

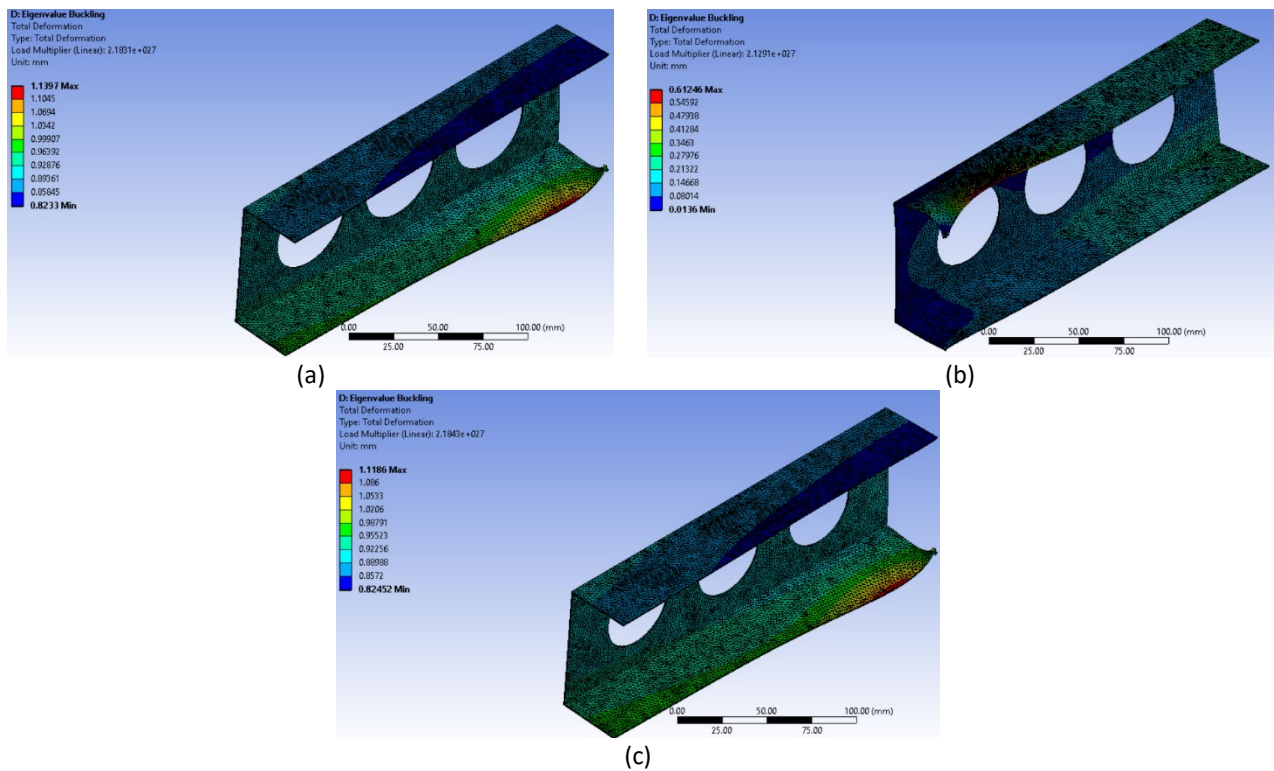


Fig. 8. Total deformation (Eigenvalue buckling) under thermal load for circular cut-outs (a) $W/W_o= 1.5$ (b) $W/W_o= 1.6$, (c) $W/W_o= 1.7$

In this study, three different cases were considered, with W/W_o ratios of 1.5, 1.6, and 1.7. Among these cases, the ratio of 1.5 stood out as having a higher diameter for the cut-outs compared to the other two ratios. As a result, the buckling load in this case was lower, indicating a decrease in the structural stability. However, it should be noted that the weight of the channel was also lower in this scenario. Conversely, when the diameter of the cut-outs was smaller, the buckling load increased. This suggests that a channel with a higher weight will exhibit a greater buckling load, as evidenced by the absence of cut-outs.

Additionally, when comparing different cut-out shapes, the circular cut-out demonstrated greater strength than the other two shapes. This advantage stems from the absence of sharp edges in the circular cut-out, which helps distribute the stress more evenly and enhances structural integrity. On the other hand, the square cut-out, characterized by 90-degree angles, is more prone to immediate structural failure due to the presence of stress concentration points.

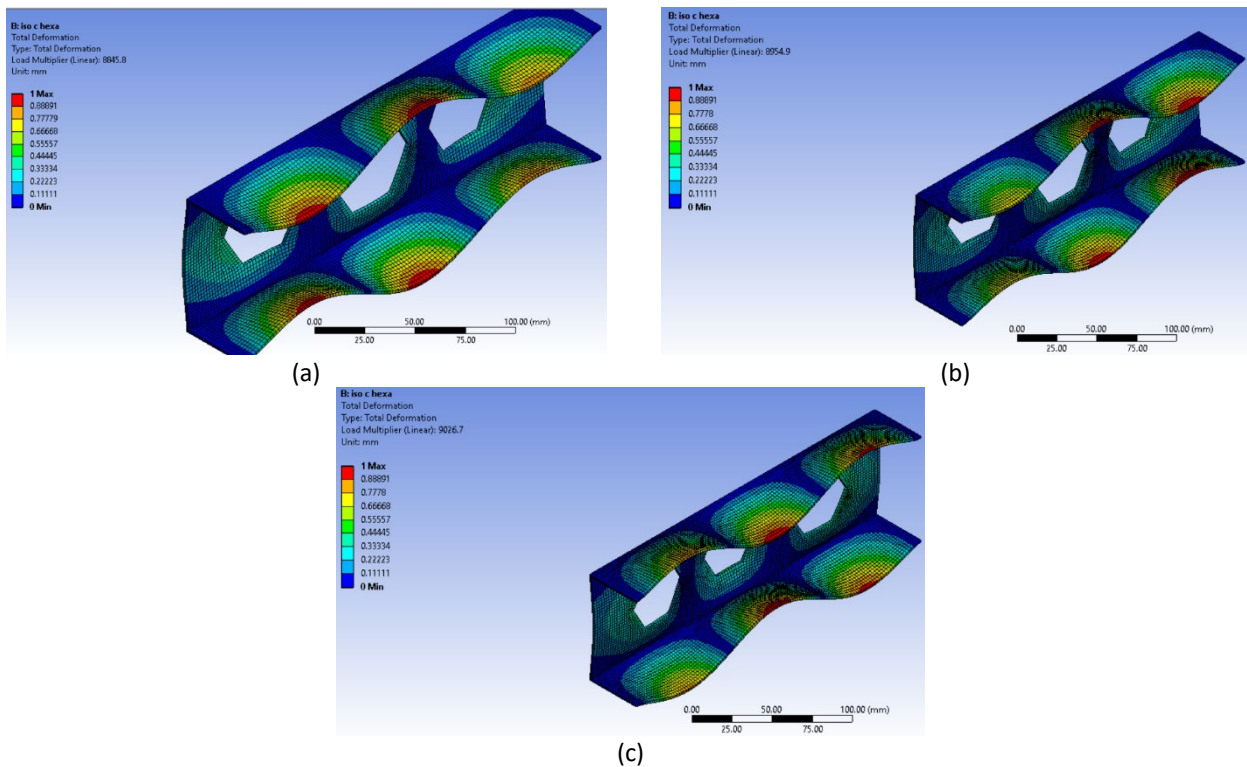


Fig. 9. Total deformation (Eigenvalue buckling) under mechanical load for hexagon cut-outs (a) $W/W_o=1.5$ (b) $W/W_o=1.6$ (c) $W/W_o=1.7$

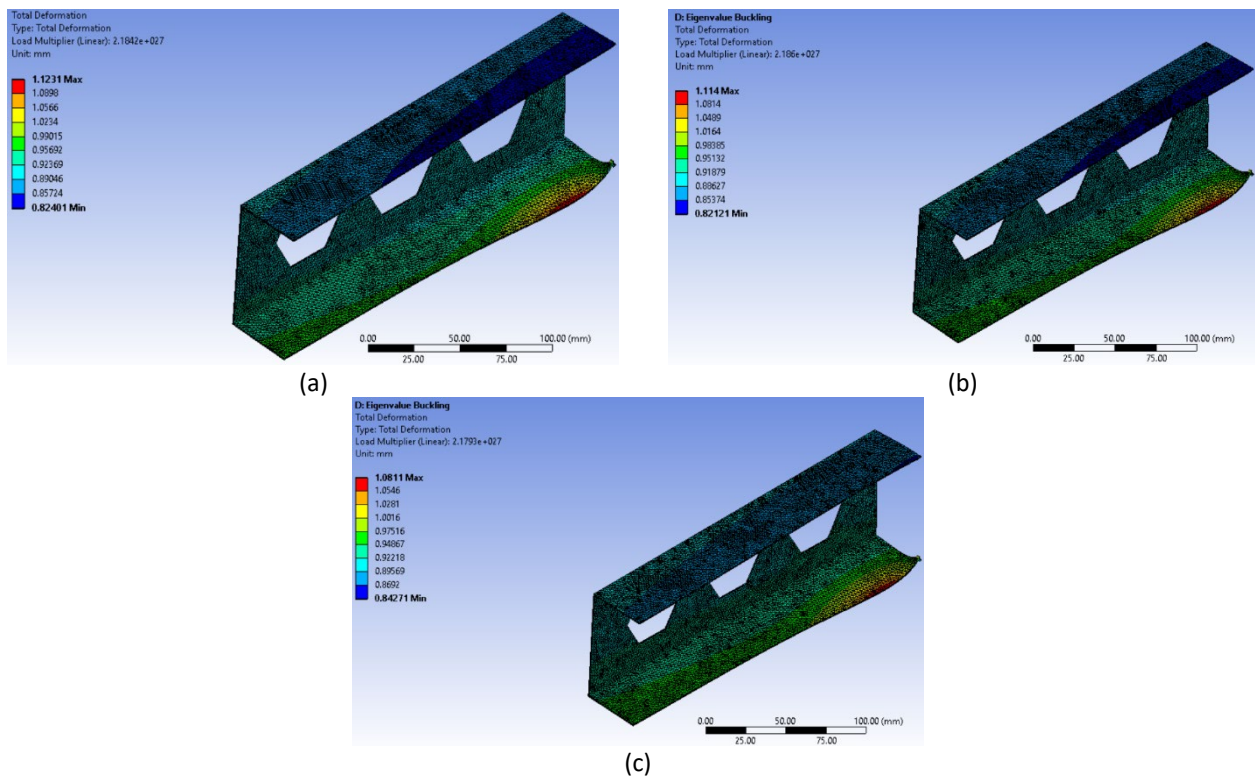


Fig. 10. Total deformation (Eigenvalue buckling) under thermal load for hexagon cut-outs (a) $W/W_o = 1.5$ (b) $W/W_o = 1.6$ (c) $W/W_o = 1.7$

In all the models, the flanges exhibited a half-wave deformation along the longitudinal axes. This deformation can be attributed to the compressive stresses that occur on the flange plane during the loading process. In the reference model (the model without any holes), local buckling was clearly observed along the web, while in the perforated models, buckling was also observed near the edges of the holes.

Across all models, Euler buckling load was observed as the first mode of buckling along the web and flanges. Despite the presence of perforations and their shapes for quasi-isotropic materials, a consistent pattern of half-wave deformation was observed. Therefore, it can be concluded that the critical buckling load and the buckling shape of the thin-wall structure are influenced by the configuration of the laminate, resulting in different behaviour.

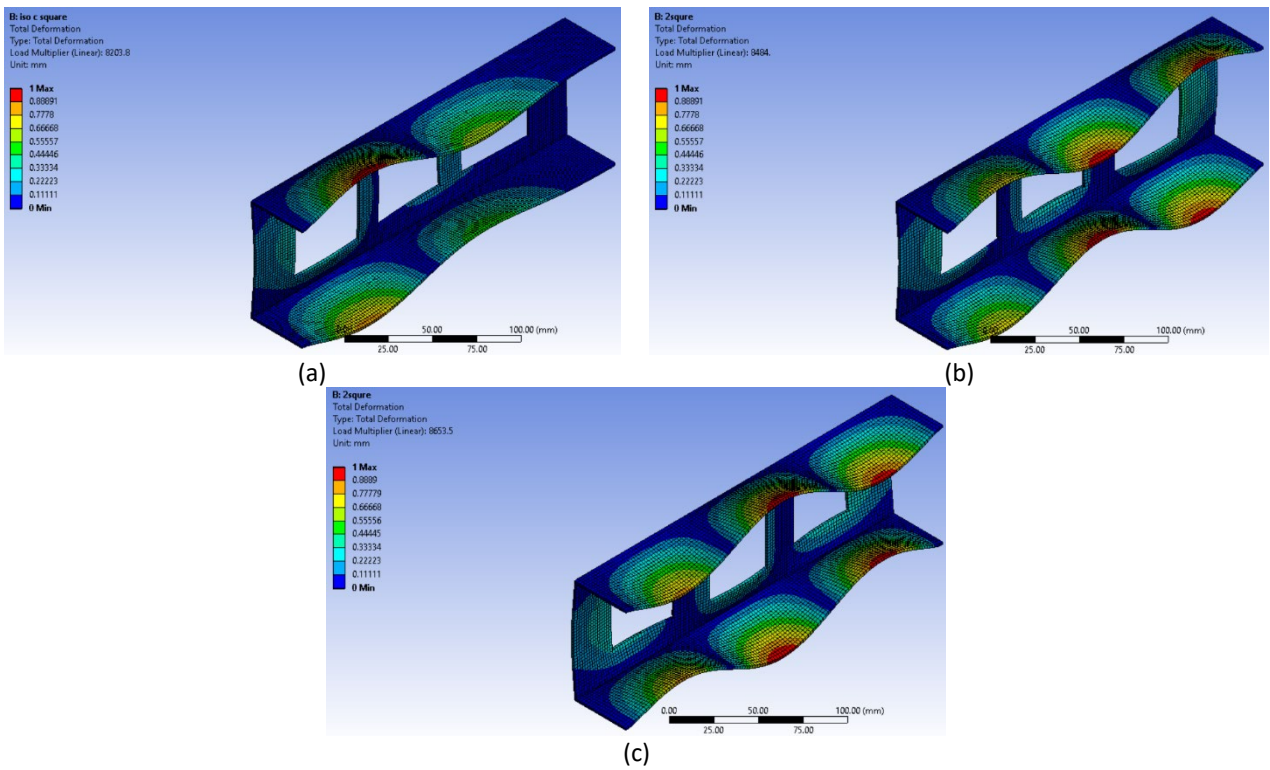


Fig. 11. Total deformation (Eigenvalue buckling) under mechanical load for square cut-outs (a) $W/W_o = 1.5$ (b) $W/W_o = 1.6$ (c) $W/W_o = 1.7$

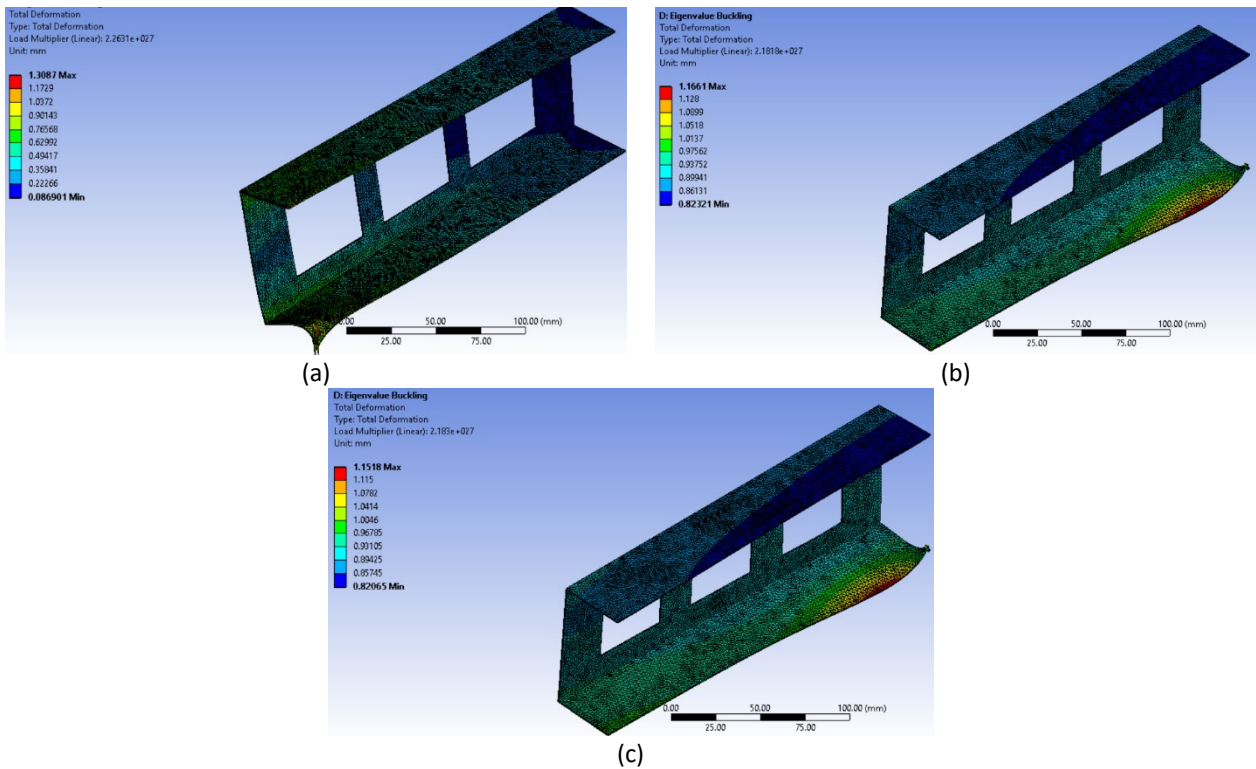


Fig. 12. Total deformation (Eigenvalue buckling) under thermal load for square cut-outs (a) $W/W_o = 1.5$ (b) $W/W_o = 1.6$ (c) $W/W_o = 1.7$

4.4 Critical Buckling Load

In Figure 13, the impact of different cut-out shapes with various laminates is depicted, while maintaining a constant spacing and opening ratio. As the cut-outs are introduced, there is a decrease in the buckling load. Among the cut-out shapes, the circular cut-out exhibits the highest critical buckling load, whereas the square cut-out has the lowest buckling load capacity. The reduction in load is particularly noticeable with the introduction of holes. This can be attributed to a greater removal of area on the web of the thin wall, with the circular shape resulting in the least amount of area removed. Furthermore, when subjected to mechanical or thermal loads, the square cut-out shape demonstrates the lowest buckling load.

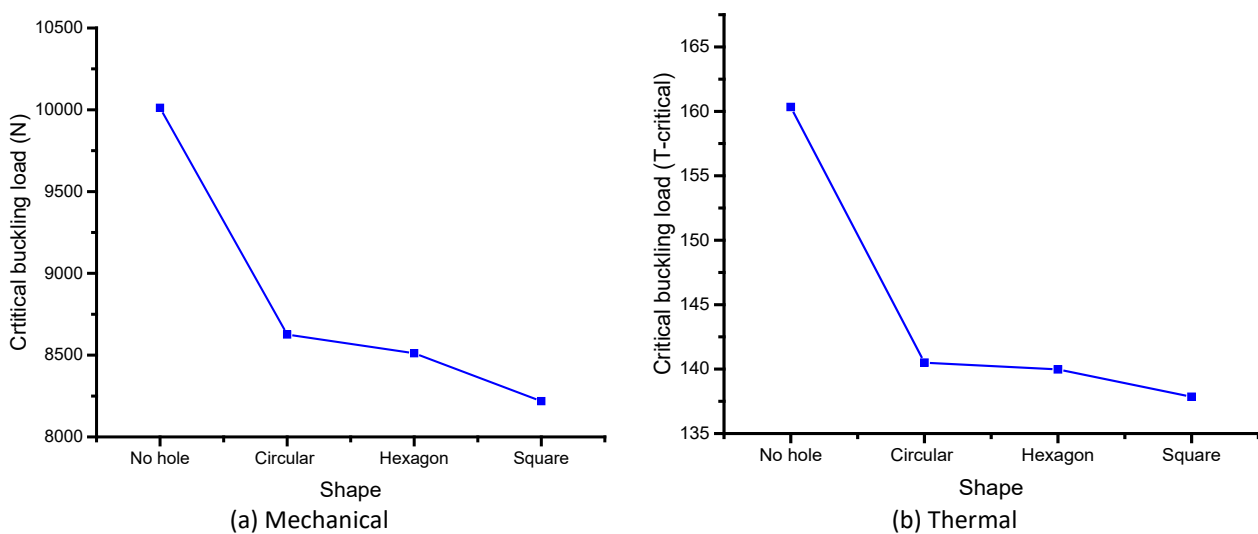


Fig. 13. Effect of hole shapes on critical buckling load for different laminates

Figure 14 illustrates a declining trend as the ratio of the opening decreases. This indicates that as the ratio decreases, the size of the hole's increases. This finding aligns with the observation made in the previous paragraph, where the introduction of greater perforation onto the web of the thin wall GFRP composite member led to a decrease in the buckling load.

In all cases studied, the mechanical load resulted in the highest buckling load values, while the thermal load exhibited the lowest range of buckling load. However, Figure 14(a) reveals that the critical buckling load remains relatively constant. Under thermal load conditions which is shown in Figure 14(b), the spacing ratio of 1.5 demonstrates higher buckling values. This occurs when the diameter is in a low range, while the body of the structure contains a high proportion of solid regions.

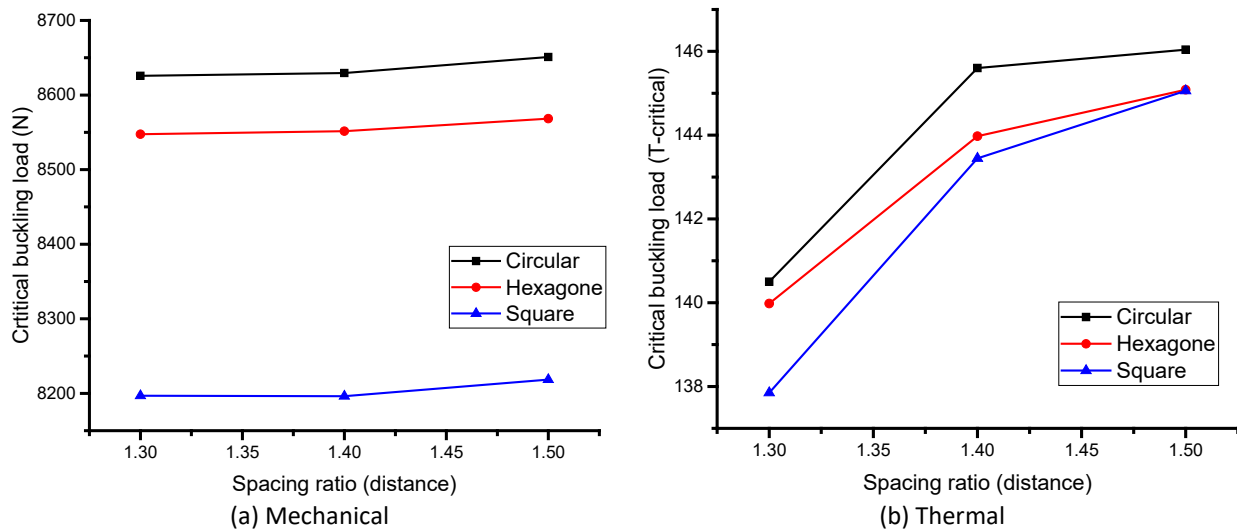


Fig. 14. Effect of spacing ratio on critical buckling load for different laminates

Finally, Figure 15 displays graphs that indicate a relatively insignificant decrease in trend as the opening ratio decreases. When the opening ratio remains constant, it can be inferred that the distance between the centres of two holes decreases as the ratio decreases. Considering all the figures mentioned in this section, it can be concluded that, across all laminates, the combination of a circular shape, an opening ratio of 1.7, and a spacing ratio of 1.5 exhibits the highest critical buckling load. This phenomenon holds true for both mechanical and thermal loads. When the distance within the structure is large, the buckling load is found to be higher. Conversely, when the distance is reduced, the buckling load decreases. However, the combined effect of these parameters will be further discussed in subsequent sections.

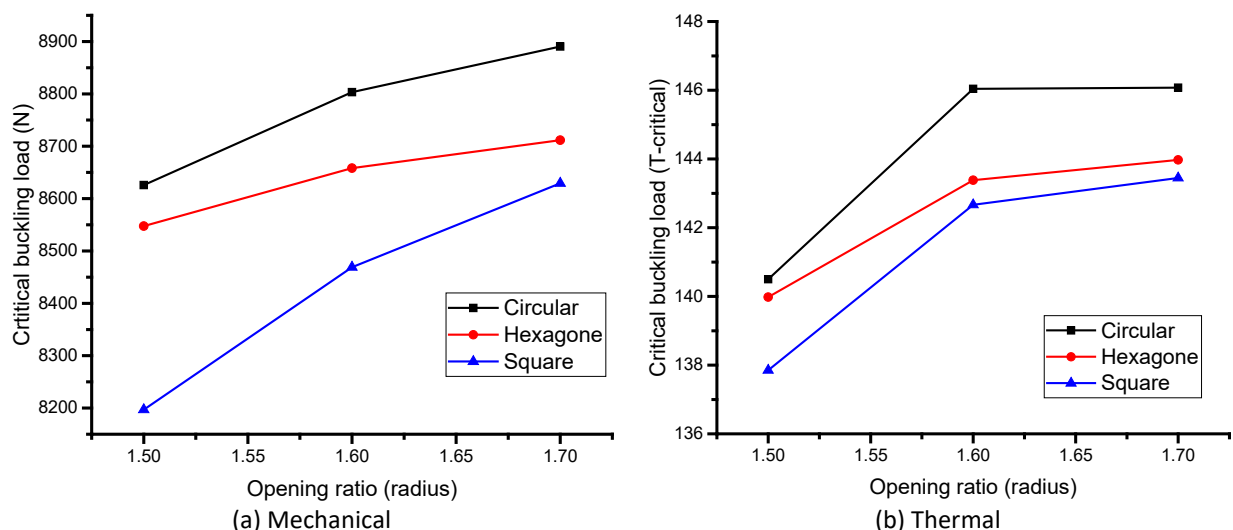


Fig. 15. Effect of opening ratio on critical buckling load for different laminates

5. Conclusion

This study compares the buckling behaviour of a thin-walled C-section channel under mechanical and thermal loads, with and without holes, using finite element analysis. Critical buckling load factors and mode shapes are investigated for both cases. Results indicate that holes significantly influence the buckling behaviour, with distinct mode shapes for each scenario. The C-section channel with

holes has a lower critical buckling load factor, indicating increased buckling risk. This underscores the need to consider holes in C-section channel design. The study enhances comprehension of buckling in thin-walled structures under mechanical and thermal loads, highlighting the importance of hole presence in C-section channel design. Findings can enhance design and optimization of C-section channels and similar structures under thermal loading. It is recommended that future research could explore diverse hole types and their impact on buckling behaviour in thin-walled structures, leading to more comprehensive design guidelines and improved structural performance.

Acknowledgement

This research was supported by the Ministry of Education of Malaysia (MOE) through the Fundamental Research Grant Scheme (FRGS/1/2022/TK04/UIAM/02/14).

References

- [1] Aabid, Abdul, Meftah Hrairi, Ahmed Abuzaid, and Jaffar Syed Mohamed Ali. "Estimation of stress intensity factor reduction for a center-cracked plate integrated with piezoelectric actuator and composite patch." *Thin-Walled Structures* 158 (2021): 107030. <https://doi.org/10.1016/j.tws.2020.107030>
- [2] Aabid, Abdul, Meftah Hrairi, Syed Jaffar Mohamed Ali, and Yasser E. Ibrahim. "Review of Piezoelectric Actuator Applications in Damaged Structures: Challenges and Opportunities." *ACS omega* 8, no. 3 (2023): 2844-2860. <https://doi.org/10.1021/acsomega.2c06573>
- [3] Aabid, Abdul, Bisma Parveez, Md Abdul Raheman, Yasser E. Ibrahim, Asraar Anjum, Meftah Hrairi, Nagma Parveen, and Jalal Mohammed Zayan. "A review of piezoelectric material-based structural control and health monitoring techniques for engineering structures: Challenges and opportunities." In *Actuators*, vol. 10, no. 5, p. 101. MDPI, 2021. <https://doi.org/10.3390/act10050101>
- [4] Bin Kamarudin, Mohamad Norfaieqwan, Jaffar Syed Mohamed Ali, Abdul Aabid, and Yasser E. Ibrahim. "Buckling analysis of a thin-walled structure using finite element method and design of experiments." *Aerospace* 9, no. 10 (2022): 541. <https://doi.org/10.3390/aerospace9100541>
- [5] Zhu, Shuhua, Jiayi Yan, Zhi Chen, Mingbo Tong, and Yuequan Wang. "Effect of the stiffener stiffness on the buckling and post-buckling behavior of stiffened composite panels—Experimental investigation." *Composite structures* 120 (2015): 334-345. <https://doi.org/10.1016/j.compstruct.2014.10.021>
- [6] Ma, Wenliang, Zihan Sun, Han Wu, Leige Xu, Yong Zeng, Yanxing Wang, and Guangyin Huang. "Buckling Analysis of Thin-Walled Circular Shells under Local Axial Compression using Vector Form Intrinsic Finite Element Method." *Metals* 13, no. 3 (2023): 564. <https://doi.org/10.3390/met13030564>
- [7] Wang, Bo, Musen Yang, Dajuan Zeng, Peng Hao, Gang Li, Ye Liu, and Kuo Tian. "Post-buckling behavior of stiffened cylindrical shell and experimental validation under non-uniform external pressure and axial compression." *Thin-Walled Structures* 161 (2021): 107481. <https://doi.org/10.1016/j.tws.2021.107481>
- [8] Czapski, Paweł, and Alexander JG Lunt. "The influence of manufacturing on the buckling performance of thin-walled, channel-section CFRP profiles—An experimental and numerical study." *Thin-Walled Structures* 184 (2023): 110475. <https://doi.org/10.1016/j.tws.2022.110475>
- [9] Abadi, P. Mouri Sardar, Abrar H. Baluch, T. A. Sebaey, D. Peeters, M. Barzegar, and C. S. Lopes. "Dispersed-ply design and optimization to improve the brittle flexural behaviour of composite laminates." *Composites Part A: Applied Science and Manufacturing* 164 (2023): 107277. <https://doi.org/10.1016/j.compositesa.2022.107277>
- [10] Ahmed, Omar Shabbir, Abdul Aabid, Jaffar Syed Mohamed Ali, Meftah Hrairi, and Norfazrina Mohd Yatim. "Progresses and Challenges of Composite Laminates in Thin-Walled Structures: A Systematic Review." *ACS omega* 8, no. 34 (2023): 30824-30837. <https://doi.org/10.1021/acsomega.3c03695>
- [11] Kumar, R. R., T. Mukhopadhyay, K. M. Pandey, and S. Dey. "Stochastic buckling analysis of sandwich plates: the importance of higher order modes." *International Journal of Mechanical Sciences* 152 (2019): 630-643. <https://doi.org/10.1016/j.ijmecsci.2018.12.016>
- [12] Guo, Shijun, Daochun Li, Xiang Zhang, and Jinwu Xiang. "Buckling and post-buckling of a composite C-section with cutout and flange reinforcement." *Composites Part B: Engineering* 60 (2014): 119-124. <https://doi.org/10.1016/j.compositesb.2013.12.055>
- [13] Seidi, J., S. M. R. Khalili, and K. Malekzadeh. "Temperature-dependent buckling analysis of sandwich truncated conical shells with FG facesheets." *Composite Structures* 131 (2015): 682-691. <https://doi.org/10.1016/j.compstruct.2015.04.068>

- [14] Han, Quanfeng, Zewu Wang, David H. Nash, and Peiqi Liu. "Thermal buckling analysis of cylindrical shell with functionally graded material coating." *Composite Structures* 181 (2017): 171-182. <https://doi.org/10.1016/j.compstruct.2017.08.085>
- [15] Kadoli, Ravikiran, and N. Ganesan. "Buckling and free vibration analysis of functionally graded cylindrical shells subjected to a temperature-specified boundary condition." *Journal of sound and vibration* 289, no. 3 (2006): 450-480. <https://doi.org/10.1016/j.jsv.2005.02.034>
- [16] Kim, Nam-II, Dong Ku Shin, and Moon-Young Kim. "Exact lateral buckling analysis for thin-walled composite beam under end moment." *Engineering Structures* 29, no. 8 (2007): 1739-1751. <https://doi.org/10.1016/j.engstruct.2006.09.017>
- [17] Nguyen, Hien Luong T., I. Elishakoff, and Vinh T. Nguyen. "Buckling under the external pressure of cylindrical shells with variable thickness." *International Journal of Solids and Structures* 46, no. 24 (2009): 4163-4168. <https://doi.org/10.1016/j.ijsolstr.2009.07.025>
- [18] Wang, Shanshuai, Shuhui Li, and Ji He. "Buckling behavior of sandwich hemispherical structure considering deformation modes under axial compression." *Composite Structures* 163 (2017): 312-324. <https://doi.org/10.1016/j.compstruct.2016.12.050>
- [19] Zhao, Cheng, Jialun Niu, Qingzhao Zhang, Chunfeng Zhao, and Junfei Xie. "Buckling behavior of a thin-walled cylinder shell with the cutout imperfections." *Mechanics of Advanced Materials and Structures* 26, no. 18 (2019): 1536-1542. <https://doi.org/10.1080/15376494.2018.1444225>
- [20] Jiao, Peng, Zhiping Chen, He Ma, Peng Ge, Yanan Gu, and Hao Miao. "Buckling behaviors of thin-walled cylindrical shells under localized axial compression loads, Part 1: Experimental study." *Thin-Walled Structures* 166 (2021): 108118. <https://doi.org/10.1016/j.tws.2021.108118>
- [21] Abedin, Nur Diana Zainal, Jaffar Syed Mohamed Ali, Abdul Aabid, and Yulfian Aminanda. "Study on the lateral torsional buckling of composite thin-walled beam." In *AIP Conference Proceedings*, vol. 2643, no. 1. AIP Publishing, 2023. <https://doi.org/10.1063/5.0112499>
- [22] Ali, Jaffar Syed Mohamed, Wan Muhammad Hafizuddin W. Embong, and Abdul Aabid. "Effect of Cut-Out Shape on the Stresses in Aircraft Wing Ribs under Aerodynamic Load." *CFD Letters* 13, no. 11 (2021): 87-94. <https://doi.org/10.37934/cfdl.13.11.8794>
- [23] Doan, Quoc Hoan, Duc-Kien Thai, and Ngoc Long Tran. "A numerical study of the effect of component dimensions on the critical buckling load of a GFRP composite strut under uniaxial compression." *Materials* 13, no. 4 (2020): 931. <https://doi.org/10.3390/ma13040931>
- [24] Rao, B. Sreenivasa, G. Sambasiva Rao, and J. Suresh Kumar. "Buckling Analysis of thin FRP laminate under Thermal Loading." *Materials Today: Proceedings* 2, no. 4-5 (2015): 3093-3099. <https://doi.org/10.1016/j.matpr.2015.07.256>